

14 MAR 23 1998

SANDIA REPORT

SAND97-2321 • UC-405

Unlimited Release

Printed September 1997

RECEIVED

MAR 27 1998

OSTI

Orthogonal Spectra and Cross Sections: Application to Optimization of Multi- Spectral Absorption and Fluorescence Lidar

DISTRIBUTION OF THIS DOCUMENT IS UNLIMITED

PF

Isaac R. Shokair

Prepared by
Sandia National Laboratories
Albuquerque, New Mexico 87185 and Livermore, California 94550

Sandia is a multiprogram laboratory operated by Sandia Corporation,
a Lockheed Martin Company, for the United States Department of
Energy under Contract DE-AC04-94AL85000.

Approved for public release; further dissemination unlimited.



Sandia National Laboratories

DTIC QUALITY INSPECTED

MASTER

SF2900Q(8-81)

19980507 013

Issued by Sandia National Laboratories, operated for the United States Department of Energy by Sandia Corporation.

NOTICE: This report was prepared as an account of work sponsored by an agency of the United States Government. Neither the United States Government nor any agency thereof, nor any of their employees, nor any of their contractors, subcontractors, or their employees, makes any warranty, express or implied, or assumes any legal liability or responsibility for the accuracy, completeness, or usefulness of any information, apparatus, product, or process disclosed, or represents that its use would not infringe privately owned rights. Reference herein to any specific commercial product, process, or service by trade name, trademark, manufacturer, or otherwise, does not necessarily constitute or imply its endorsement, recommendation, or favoring by the United States Government, any agency thereof, or any of their contractors or subcontractors. The views and opinions expressed herein do not necessarily state or reflect those of the United States Government, any agency thereof, or any of their contractors.

Printed in the United States of America. This report has been reproduced directly from the best available copy.

Available to DOE and DOE contractors from
Office of Scientific and Technical Information
P.O. Box 62
Oak Ridge, TN 37831

Prices available from (615) 576-8401, FTS 626-8401

Available to the public from
National Technical Information Service
U.S. Department of Commerce
5285 Port Royal Rd
Springfield, VA 22161

NTIS price codes
Printed copy: A03
Microfiche copy: A01



Orthogonal Spectra and Cross Sections: Application to Optimization of Multi-Spectral Absorption and Fluorescence Lidar

Isaac R. Shokair
Pulsed Power and Laser Initiatives Department
Sandia National Laboratories
P. O. Box 5800
Albuquerque, New Mexico 87185-1188

Abstract

This report addresses the problem of selection of lidar parameters, namely wavelengths for absorption lidar and excitation/fluorescence pairs for fluorescence lidar, for optimal detection of species. Orthogonal spectra and cross sections are used as mathematical representations which provide a quantitative measure of species distinguishability in mixtures. Using these quantities, a simple expression for the absolute error in calculated species concentration is derived and optimization is accomplished by variation of lidar parameters to minimize this error. It is shown that the optimum number of wavelengths for detection of a species using absorption lidar (excitation/fluorescence pairs for fluorescence lidar) is the same as the number of species in the mixture. Each species present in the mixture has its own set of optimum wavelengths. There is usually some overlap in these sets. The optimization method is applied to two examples, one using absorption and the other using fluorescence lidar, for analyzing mixtures of four organic compounds. The effect of atmospheric attenuation is included in the optimization process. Although the number of optimum wavelengths might be small, it is essential to do large numbers of measurements at these wavelengths in order to maximize canceling of statistical errors.

Acknowledgment

The author wishes to thank Perry Gray, Phil Hargis, Al Lang, Marshall Lapp, Stephen Rosenthal and John Wagner for useful discussions and comments. This work was supported by the Department of Energy under Contract No. DE-AC04-94AL85000.

Contents

I. Introduction	7
II. Formalism for Orthogonal Spectra and Cross Sections - Measure of Species	
Distinguishability	8
III. Optimization of Lidar Parameters	12
IV. Optimized Wavelengths for Absorption Lidar	16
V. Optimized Detection for Fluorescence Lidar	20
VI. Summary	23
VII. References	30

I. Introduction

For multispectral lidar systems, target identification can be accomplished using return fluorescence or absorption spectra at multiple laser excitation wavelengths⁽¹⁻⁴⁾. For a UV absorption lidar for example, the drop in the elastic backscatter intensity across a gaseous plume, at several properly chosen excitation wavelengths, can be used to calculate the concentrations of species in the plume. Similarly, signals scattered off topographic targets at several wavelengths can be used for chemical analysis of plumes in both the IR and UV ranges. Return fluorescence spectra from gaseous plumes and solid targets can also be used for species identification and concentration calculation.

For conventional differential absorption lidar (DIAL), a chemical species can be identified in the presence of other unknown species if the species of interest has two adjacent wavelengths, one with strong and the other with weak absorption (on-off wavelengths). The assumption is that the on-off wavelengths are sufficiently close that other species have nearly uniform absorption cross sections in that region. When this is not the case, all the possible species have to be represented by their absorption spectra and enough wavelengths chosen in order to be able to unfold the absorption pattern and calculate species concentrations. The minimum number of wavelengths is equal to the number of species present for a lidar which utilizes range resolved atmospheric scattering or topographic scattering. A minimum of one additional wavelength is needed for a lidar which uses topographic scattering off a target with unknown ratio of the on-plume to off-plume albedo, assuming that this ratio is independent of wavelength.

For multispectral fluorescence lidar, laser light at several excitation wavelengths induces fluorescence in gaseous plumes or surfaces of solid or liquid targets. The detected fluorescence can be spectrally resolved or integrated over specified wavelength bands. Again as in the case for absorption lidar, the minimum number of excitation/fluorescence pairs is the number of possible species present. Fluorescence lidar can also be used in a differential absorption mode to detect certain species in the presence of other unknown species. As in the case for DIAL, this relies on the existence of on-off wavelengths which are sufficiently close for the species of interest so that other species can be assumed to have constant parameters in this wavelength range. Instead of the absorption cross section, the product of the absorption cross section and the fluorescence yield should be used to determine on-off wavelengths in this case.

For some species with distinct absorption or fluorescence features, the choice of laser wavelengths and fluorescence bands can be obvious. For other species with broad spectral features, or as the number of possible species increases, choosing the lidar parameters is a non-trivial matter. One possible method for choosing these parameters is by using genetic algorithms⁽⁵⁻⁶⁾. In these algorithms many different sets of lidar parameters are allowed to compete and ones with higher fitness values are allowed to survive and reproduce new generations, while ones with low fitness values die out. The fitness of a particular set of lidar parameters is defined as a function of the difference between known and calculated concentrations using training data which is either measured or computer simulated. Noise is usually added to computer generated data during the training process. In general, genetic algorithms are expected to be significantly more efficient than random searches.

Another possible method of optimization of lidar parameters is through the use of orthogonal spectra and cross sections. This is the subject of this report. These quantities provide a quantitative measure of species distinguishability and can be used to maximize the detection capability for a given species in the presence of many others. In the second section of this report the formalism for orthogonal spectra and cross sections is developed and the mathematical equivalence of the absorption and fluorescence cases is established. Solutions for species concentrations in terms of the orthogonal quantities are also obtained and a connection is made with the partial least squares method. The problem of optimization is then discussed in section III and quantities appropriate for optimization are given. In the last two sections we consider two examples of parameter selection for both absorption and fluorescence lidar and discuss how the effect of atmospheric attenuation can be included in the optimization process. In all of the analysis presented in this report the assumption is made that the relation between measured quantities and species concentrations is linear. For the absorption case this is true for all concentrations, however for the fluorescence case it is only true for small optical thickness. Finite optical thickness effects can be included in the optimization process to some extent by applying the appropriate distortions to the measured spectra in the desired concentration ranges.

The analysis presented in this report assumes that all possible species in a mixture are represented by their absorption cross sections or fluorescence spectra. The situation of identification of a specific species in a mixture that contains other species with completely unknown spectra is not addressed in this report. Such situations can be addressed by factor analysis methods, if calibration data, including the unknown species, is available.

II. Formalism for Orthogonal Spectra and Cross Sections - Measure of Component Distinguishability

For multispectral absorption lidar and fluorescence lidar, in the limit of small optical thickness, the relation between measured quantities and species concentrations is linear. For the case of absorption using the range resolved elastic backscatter intensity, the ratio of the intensity after the plume to before the plume is the two way transmission coefficient across the plume and is given by:

$$\rho(\lambda_i) = \exp \left[-2 \sum_k \sigma_k(\lambda_i) C_k \right], \quad (1)$$

where $\sigma_k(\lambda_i)$ is the absorption cross section of the k -th species at the excitation wavelength λ_i , and C_k is the line integrated density across the plume for the k -th species:

$$C_k = \int_{\text{plume}} dx N_k(x),$$

where $N_k(x)$ is the density profile. The factor of two in Eq. (1) is because of the assumption that both source and detector are at the same location and thus detected scattered light from behind the plume travels twice across the plume. Equation (1) also assumes that the plume is narrow enough so that

atmospheric attenuation across the plume is negligible. If this is not the case, a correction for atmospheric attenuation should be applied. Equation (1) can be written in linear form as:

$$R(\lambda_i) \equiv -\frac{1}{2} \ln[\rho(\lambda_i)] = \sum_k \sigma_k(\lambda_i) C_k, \quad (2)$$

Since the lidar system usually has more excitation wavelengths than unknown chemical components, Eq. (2) can be solved for the concentrations using a linear least squares solution method.

For optically thin plumes, the fluorescence resulting from laser excitation is nearly linear in the concentrations and thus the spectrum of a mixture can be written as a linear combination of individual spectral components, that is:

$$M(\lambda_i, \lambda_j) = \sum_k C_k S_k(\lambda_i, \lambda_j) \quad (3)$$

where λ_i and λ_j denote the excitation and fluorescent wavelengths respectively, M is the mixture spectrum and S_k is the spectrum for the k -th component, which is the product of the absorption cross section, quantum yield (taking quenching into account) and the spectral shape function. Equation (3) needs to be corrected for atmospheric attenuation and other factors depending on the application and could also represent fluorescence integrated over a certain time gate. Again, since the number of equations represented by Eq. (3) is usually much larger than the number of unknown species, linear least squares minimization can be used to obtain solutions for the concentrations. Equation (3) is mathematically equivalent to Eq. (2) since each pair (λ_i, λ_j) represents a single spectral value, and thus the results obtained from the absorption case are directly applicable to the linear fluorescence case.

The degree of distinguishability of two components can be defined as the part of one component that is linearly independent of the other. Thus if $\underline{\sigma}_1$ and $\underline{\sigma}_2$ are the spectra or cross sections of two species (note $\underline{\sigma}_k$ is a vector quantity represented by $\underline{\sigma}_k = (\sigma_{k1}, \sigma_{k2}, \dots, \sigma_{kn})$, where σ_{kj} is the cross section for the k -th species and j -th wavelength, or j -th excitation/fluorescence pair for fluorescence), the part of $\underline{\sigma}_2$ that is distinguishable from $\underline{\sigma}_1$ can be written as:

$$\hat{\underline{\sigma}}_2 = \underline{\sigma}_2 - \mu \underline{\sigma}_1 \quad (4)$$

where the constant μ is chosen such that the norm of $\hat{\underline{\sigma}}_2$ is minimized. If the norm is defined in the normal manner, $|\hat{\underline{\sigma}}_2|^2 = \sum_j (\hat{\sigma}_{2j})^2$, the constant μ is found from the condition that $\partial |\hat{\underline{\sigma}}_2|^2 / \partial \mu = 0$ and is given by:

$$\mu = \sum_j \sigma_{2j} \sigma_{1j} / \sum_j (\sigma_{1j})^2 \quad (5)$$

Define the inner product of two vector quantities in the normal manner: $\langle \underline{\sigma}_1, \underline{\sigma}_2 \rangle \equiv \sum_j \sigma_{1j} \sigma_{2j}$. In terms of this inner product we have: $\mu = \langle \underline{\sigma}_1, \underline{\sigma}_2 \rangle / \langle \underline{\sigma}_1, \underline{\sigma}_1 \rangle$. It is also readily seen that $\langle \hat{\underline{\sigma}}_2, \underline{\sigma}_1 \rangle = 0$, that is, $\hat{\underline{\sigma}}_2$ is orthogonal to $\underline{\sigma}_1$ and thus the part of $\underline{\sigma}_2$ that is distinguishable from $\underline{\sigma}_1$ is the component of $\underline{\sigma}_2$ which is orthogonal to $\underline{\sigma}_1$. This formalism can be generalized to multiple species as follows. New spectra (or cross sections) can be defined as:

$$\begin{aligned}\hat{\underline{\sigma}}_1 &= \underline{\sigma}_1 \\ \hat{\underline{\sigma}}_2 &= \underline{\sigma}_2 - \mu_{21} \hat{\underline{\sigma}}_1 \\ \hat{\underline{\sigma}}_3 &= \underline{\sigma}_3 - \mu_{32} \hat{\underline{\sigma}}_2 - \mu_{31} \hat{\underline{\sigma}}_1 \\ &\vdots \\ \hat{\underline{\sigma}}_N &= \underline{\sigma}_N - \mu_{N,N-1} \hat{\underline{\sigma}}_{N-1} - \cdots - \mu_{N1} \hat{\underline{\sigma}}_1\end{aligned}\tag{6}$$

where the constants μ_{kl} are chosen to minimize the respective norms. Following the same procedure outlined for the two component case we find:

$$\begin{aligned}\mu_{kl} &= \langle \underline{\sigma}_k, \hat{\underline{\sigma}}_l \rangle / \langle \hat{\underline{\sigma}}_l, \hat{\underline{\sigma}}_l \rangle \quad k > l \\ \langle \hat{\underline{\sigma}}_k, \hat{\underline{\sigma}}_l \rangle &= 0 \quad k \neq l\end{aligned}\tag{7}$$

Similarly the orthogonality conditions could be used to obtain the above values of μ and could be shown to result in minimized norms. We note that the order of species 1 thru $N-1$ in Eq. (6) is not important and any ordering would result in the same value for $\hat{\underline{\sigma}}_N$, which is the species of interest for the subsequent analysis. This is a result of the fact that $\hat{\underline{\sigma}}_N$ is orthogonal to the spectra for species 1 thru $N-1$ or any linear combination of these spectra. If we define $\mu_{kk} = 1$, and $\mu_{kl} = 0$ for $k < l$, Eq. (6) can be written as:

$$\underline{\sigma}_k = \sum_{l=1}^N \mu_{kl} \hat{\underline{\sigma}}_l \quad k = 1, \dots, N\tag{8}$$

where N is the total number of species being considered. Equation (8) holds for all the wavelengths and can be written in matrix form as:

$$\underline{\underline{\sigma}} = \underline{\mu} \cdot \hat{\underline{\underline{\sigma}}}\tag{9}$$

where the k -th rows of the matrices $\underline{\underline{\sigma}}$ and $\hat{\underline{\underline{\sigma}}}$ represent the spectra and the orthogonal spectra for the

k -th species at the different wavelengths and $\underline{\underline{\mu}}$ is the triangular matrix given by:

$$\begin{pmatrix} 1 & 0 & \cdots & \cdots & 0 \\ \underline{\mu}_{21} & 1 & 0 & \cdots & 0 \\ \underline{\mu}_{31} & \underline{\mu}_{32} & 1 & 0 & \cdots & 0 \\ \vdots & & & & & \\ \vdots & & & & & \\ \underline{\mu}_{N1} & \underline{\mu}_{N2} & \underline{\mu}_{N3} & \cdots & & 1 \end{pmatrix}.$$

The orthogonality condition given by Eq. (7) implies that the product $\underline{\underline{\sigma}} \cdot \underline{\underline{\sigma}}^T$ is a diagonal matrix, that is, $\underline{\underline{\sigma}}$ is the product of a diagonal matrix and an orthogonal matrix. The above procedure is identical to the Gram-Schmidt orthogonalization procedure for finite dimensional spaces and amounts to orthogonalization of a matrix.

If we write equation (2) or (3) in terms of the orthogonal spectra, the solution for the N -th species is readily apparent as we now show. Using equation (8) in Eq. (1) we have:

$$\begin{aligned} R_i &= \sum_{k=1}^N \left(\sum_{l=1}^N \underline{\mu}_{kl} \hat{\sigma}_{li} \right) C_k \\ &= \sum_{l=1}^N \xi_l \hat{\sigma}_{li} \end{aligned} \tag{10}$$

where new variables are defined as:

$$\xi_l = \sum_{k=1}^N \underline{\mu}_{kl} C_k \tag{11}$$

Taking the inner product of Eq. (10) with $\hat{\sigma}_m$ and using orthogonality, we obtain:

$$\xi_m = \langle R, \hat{\sigma}_m \rangle / \langle \hat{\sigma}_m, \hat{\sigma}_m \rangle \tag{12}$$

Once the vector ξ is determined, the concentrations can be readily found using back substitution in Eq. (11). It should be noted that this solution is identical to the solution obtained by direct least squares solution of Eq. (2), since Eq. (10) is identical to Eq. (2) and the minimized quantities are the same.

Note also that minimizing $\chi^2 = \sum_i \left[R_i - \sum_{l=1}^N \xi_l \hat{\sigma}_{li} \right]^2$ also results in Eq. (12). Now the advantage of using the orthogonal representation becomes clear. From Eq. (11) and the definition of the matrix μ we can immediately write the solution for the concentration of the N-th species as:

$$\begin{aligned} \xi_N &= C_N \\ &= \langle \underline{R}, \hat{\underline{\sigma}}_N \rangle / \langle \hat{\underline{\sigma}}_N, \hat{\underline{\sigma}}_N \rangle \end{aligned} \quad (13)$$

Thus the solution for the concentration of the last species is isolated in terms of the measured quantity $R(\lambda)$ and the orthogonal spectrum for that species, which is equivalent to a situation with a single species. Before moving to the next section which discusses optimization of the lidar system, it is important to note the connection of the result in Eq. (13) and the partial least squares and other calibration methods.

In the method of partial least squares⁽⁷⁻⁸⁾, the quantity R is measured at the wavelengths of interest for several combinations of the concentrations (training set) for which only the concentration of the species of interest need be known. If there are M sets of the measurements, we can write using Eq. (13) in matrix form for all the measurements as:

$$\begin{pmatrix} C_N^1 \\ C_N^2 \\ \vdots \\ C_N^M \end{pmatrix} = \begin{pmatrix} R_{11} & R_{12} & \cdots & \cdots & R_{1v} \\ R_{21} & R_{22} & \cdots & \cdots & R_{2v} \\ \vdots & \vdots & & & \vdots \\ \vdots & \vdots & & & \vdots \\ C_N^M & R_{M1} & R_{M2} & \cdots & \cdots & R_{Mv} \end{pmatrix} \begin{pmatrix} \hat{\sigma}_{N1} \\ \hat{\sigma}_{N2} \\ \vdots \\ \vdots \\ \hat{\sigma}_{Nv} \end{pmatrix} \frac{1}{\zeta} \quad (14)$$

where C_N^j is the concentration of the N-th species for the j-th measurement, R_{kl} is the value of R for the k-th measurement and the l-th wavelength and $\zeta = \langle \hat{\sigma}_N, \hat{\sigma}_N \rangle$. Equation (14) can be solved for the orthogonal cross sections (or spectra) assuming $M \geq v \geq N$, using least squares minimization. This can be repeated for all the species if so desired. This result is very similar to the Partial Least Squares method, and actually provides a clear way for understanding how that method works.

III. Optimization of Lidar Parameters

Depending on the particular application of the lidar system, there might be limitations imposed on the number of laser excitation wavelengths, resolution of the return fluorescence spectra, and other lidar parameters. Even without such limitations it is desirable to find optimum excitation (or absorption) wavelengths and method of analysis of the resulting data to best accomplish the mission for which the lidar system is designed. In this section we consider the problem of optimization and

consider the question of what is the number and values of the excitation and detection wavelengths which would result in optimal detection of a particular species. By optimal we mean the set of wavelengths which minimizes the error in calculated concentrations given a representation of error in measured quantities. In the following two sections specific examples for absorption and fluorescence are considered. It should be made very clear that by optimum number of wavelengths we do not mean a limit on the number of measurements or the number of data points collected, but rather a limit on the values of wavelengths used. Once an optimum set of wavelength values has been determined, as many measurements as possible need to be made at these values (or slightly different values to reduce possible systematic errors) in order to reduce effects of noise and other statistical errors. It is also possible that there might be many near optimal sets which can also be used.

As seen in the previous section of this report, given a set of N possible species, the distinguishability of the N -th species from all the others can be measured by the orthogonal spectra denoted by $\hat{\underline{\sigma}}_N$. A figure of merit of relative distinguishability for the N -th species can then be defined heuristically as:

$$\varphi = \frac{\sum_i |\hat{\sigma}_N(\lambda_i)|}{\left\{ \sum_i \sigma_k(\lambda_i) \right\}_{\text{max over species}}}$$

if the parameter φ is near zero, the spectra of the N -th species is nearly linearly dependent on the others and thus will be difficult to isolate. This of course also depends on the signal to noise ratio (SNR) for the system. If φ is of order unity, the N -th species has a relatively large linearly independent component and thus can be isolated as if it were the only species present. One can also define another figure of merit: $\psi = \sum_i |\hat{\sigma}_N(\lambda_i)| / \sum_i \sigma_N(\lambda_i)$, which is a measure of the fractional detectability of species N , in the presence of the other $N-1$ species, relative to the case where the N -th species is the only one present. Based on this discussion, the number and values of wavelengths for optimal detection of the N -th species would be the values that maximize the parameter φ , ψ , or some other measure of detectability.

A more exact criterion for optimization is to minimize resulting error in the concentration given errors in the measured quantities. From equation (13) we can write the error in the concentration δC_N in terms of measurement error δR as:

$$\delta C_N = \langle \delta R, \hat{\underline{\sigma}}_N \rangle / \langle \hat{\underline{\sigma}}_N, \hat{\underline{\sigma}}_N \rangle \quad (15)$$

One can also choose to minimize the variance of C_N , given statistical errors δR . For normal

distributions of the error δR , the variance is given by:

$$(\delta C_N)^2 = \sum_i \left(\frac{\partial C_N}{\partial R_i} \right)^2 (\delta R_i)^2 = \sum_i \frac{(\hat{\sigma}_{Ni})^2}{[\langle \hat{\sigma}_N, \hat{\sigma}_N \rangle]^2} (\delta R_i)^2$$

For the analysis in this report, minimization of the error given by Eq. (15) will be used for optimization. If δR is the measurement error due to instrument limitations, and is independent of the spectra being measured, a reasonable quantity to minimize for the general case is given by:

$$f_v = \sum_{i=1}^v |\hat{\sigma}_N(\lambda_i)| / \sum_{i=1}^v [\hat{\sigma}_N(\lambda_i)]^2 \quad (16)$$

where v is the number of wavelengths (for absorption v is the number of absorption wavelengths and for fluorescence it is the number of excitation/fluorescence wavelengths pairs). One can also choose to maximize the quantity: $\sum_i |\hat{\sigma}_N(\lambda_i)|$, which gives similar, but not identical results to minimizing f_v as given by Eq. (16).

It should be noted that both δR and $\hat{\sigma}_N$ can have positive and negative values, and thus we choose to use $|\hat{\sigma}_N|$ in Eq. (16) in order for the results to be valid for the general case. We also note that equation (16) needs to be modified to take into account wavelength dependent effects such as atmospheric attenuation, finite optical thickness, and other effects related to either the environment or the instruments. Some of these effects will be considered in the following section. The parameter f_v as given by equation (16) has some interesting properties. The first property is: Given a set of N wavelengths, $\lambda_1, \lambda_2, \dots, \lambda_N$, any set of v wavelengths ($v > N$) with $\lambda_{N+1}, \dots, \lambda_v$ being repeated values of any of the wavelengths in the set $\lambda_1, \lambda_2, \dots, \lambda_N$, the value of f_v is unchanged and is equal to f_N . The second property (which was only verified numerically for several cases, but not yet proven mathematically) is as follows: If over a specified range of wavelengths, the set of N wavelengths $\lambda_1, \lambda_2, \dots, \lambda_N$, results in a global minimum of f_N , any other set of v wavelengths will have $f_v \geq f_N$. This property implies that the absolute error as given by equation (16), is minimized by using the same number of wavelengths as the number of species present. This property seems to hold for several cases that we tested numerically, and although we do not have a mathematical proof at this point in time, we suspect that it is valid for all cases. In fact, the case with a single species and multiple wavelengths illustrates this property in a very simple manner. In this case we have f_v given from Eq. (16) by:

$$f_v = \sum_{i=1}^v |\sigma(\lambda_i)| / \sum_{i=1}^v [\sigma(\lambda_i)]^2 = \sum_{i=1}^v w_i \frac{1}{|\sigma(\lambda_i)|}, \quad w_i = \frac{[\sigma(\lambda_i)]^2}{\sum_{i=1}^v [\sigma(\lambda_i)]^2}.$$

Since from the above equation we have $\sum_{i=1}^v w_i = 1$, the quantity f_v is a minimum for $v = 1$, at the value of λ for which $\sigma(\lambda)$ is maximized. This type of argument can not be extended to the general case of multiple species because in contrast to the normal spectra, the orthogonal spectra change at all wavelengths if a new wavelength is added to the set.

The first property mentioned above can be shown by considering the definition of the orthogonal spectra. In matrix form we have in general for $v \geq N$ (see Eq. (9)): $\underline{\underline{\sigma}} = \underline{\underline{\mu}} \cdot \hat{\underline{\sigma}}$. Multiplying this equation by $\hat{\underline{\sigma}}^T$ from the right and using the orthogonality property $(\hat{\underline{\sigma}} \cdot \hat{\underline{\sigma}}^T)_{ij} = 0, i \neq j$, we obtain:

$$\underline{\underline{\mu}} = \underline{\underline{w}}^{-1} \cdot \underline{\underline{\sigma}} \cdot \hat{\underline{\sigma}}^T \quad (17)$$

where $\underline{\underline{w}}$ is a diagonal matrix with elements $w_{ii} = \langle \hat{\underline{\sigma}}_i, \hat{\underline{\sigma}}_i \rangle$. Using the fact that the last column of the matrix $\underline{\underline{\mu}}$ is all zero except $\mu_{NN} = 1$, we obtain:

$$\begin{aligned} \langle \underline{\sigma}_i, \hat{\underline{\sigma}}_N \rangle &= 0 \quad i \neq N \\ \langle \underline{\sigma}_N, \hat{\underline{\sigma}}_N \rangle &= \langle \hat{\underline{\sigma}}_N, \hat{\underline{\sigma}}_N \rangle \end{aligned} \quad (18)$$

which is just a restatement of the orthogonality condition, namely that $\hat{\underline{\sigma}}_N$ is orthogonal to any linear combination of $\underline{\sigma}_i, i = 1, \dots, N-1$. These two equations can be written as:

$$\begin{pmatrix} \sigma_{11} & \sigma_{12} & \cdots & \cdots & \sigma_{1v} \\ \vdots & & & & \\ \vdots & & & & \\ \vdots & & & & \\ \sigma_{N1} & \sigma_{N2} & \cdots & \cdots & \sigma_{Nv} \end{pmatrix} \begin{pmatrix} \hat{\sigma}_{N1} \\ \vdots \\ \hat{\sigma}_{Nv} \end{pmatrix} = \begin{pmatrix} 0 \\ \vdots \\ 0 \\ \langle \hat{\underline{\sigma}}_N, \hat{\underline{\sigma}}_N \rangle \end{pmatrix}$$

where σ_{kj} denotes the spectrum (cross section) for the k -th species and the j -th wavelength. Now consider two cases, one with $v = N$, and the other with $v = N+1$, with λ_v a repeat of one of the other wavelengths. If the wavelengths are arranged in such a way that λ_N and λ_{N+1} are equal and we use $\hat{\underline{\sigma}}_N$ for the case with $v = N$ and $\tilde{\underline{\sigma}}_N$ for case with $v = N+1$, the above system and the fact that $\tilde{\sigma}_{NN} = \tilde{\sigma}_{N,N+1}$ imply the following relation:

$$\frac{\tilde{\sigma}_{N1}}{\hat{\sigma}_{N1}} = \frac{\tilde{\sigma}_{N2}}{\hat{\sigma}_{N2}} = \dots = \frac{\tilde{\sigma}_{N,N-1}}{\hat{\sigma}_{N,N-1}} = \frac{2\tilde{\sigma}_{NN}}{\hat{\sigma}_{NN}} = \frac{\langle \tilde{\underline{\sigma}}_N, \tilde{\underline{\sigma}}_N \rangle}{\langle \hat{\underline{\sigma}}_N, \hat{\underline{\sigma}}_N \rangle} \quad (19)$$

This is a result of the fact that the two systems of equations for $\hat{\underline{\sigma}}_N$ and $\tilde{\underline{\sigma}}_N$ are identical if we replace $\hat{\sigma}_{NN}$ by $2\tilde{\sigma}_{NN}$ and $\langle \hat{\underline{\sigma}}_N, \hat{\underline{\sigma}}_N \rangle$ by $\langle \tilde{\underline{\sigma}}_N, \tilde{\underline{\sigma}}_N \rangle$. Using Eq. (19) in (16) we immediately conclude that $f_v = f_N$ for this special case. This proof can be extended to an arbitrary number of repeating wavelengths. The mathematical proof of the second property is still work in progress.

One of the implications of the second property is that for optimal detection of a species, there are N optimum values of wavelengths (N is the total number of species present) that need to be used. These wavelengths are not necessarily the same as for optimal detection of the other species and thus the analysis needs to be repeated for all species, with the species of interest being treated as the N -th species. In the solution given by equation (16), although measurements might be available at the other wavelengths, a more accurate solution could be obtained by just using the optimum set of N wavelengths for the species under consideration. Again statistical cancelling of errors requires that a large number of measurements needs to be made at these wavelengths. Another point that needs to be made is the following: Although there is a unique set of N wavelengths that minimizes f_v globally for a given species, there are possibly many other sets that result in similar values of f_v . Such multiple sets could be used to avoid possible systematic errors that might be associated with certain wavelengths.

IV. Optimized Wavelengths for Absorption Lidar

In this section we consider an example of wavelengths selection for a multispectral UV absorption lidar system for optimized detection of four aromatic compounds, benzene, m-xylene, p-xylene and toluene. The objective is to find wavelengths for optimal detection of each of these species in the presence of all the others. Using results from the previous section, we conclude that there is an optimum set of $v = 4$ wavelengths for the detection of each of these species. Absorption cross sections for these species are shown in Fig. (1). These cross sections are the result of a moving box average of experimentally measured values over a width of 0.1 nm (5 points of measured data)⁽⁹⁾. Since the cross sections are complicated functions of wavelength, the functional $f_{v=N}(\lambda_1, \lambda_2, \dots, \lambda_N)$ is expected to have multiple local minima. A simple and a very crude way of finding the global minimum is to calculate f_v for all possible combinations of N wavelengths. For the case under consideration with $N=4$, and a set of about 1500 wavelengths for each species, the total number of possibilities is roughly $1500^N/N! \approx 2 \times 10^{11}$, which is rather large. We can however significantly reduce the number of wavelengths and still maintain the general shape of the absorption cross section profiles. In Fig. (2) the cross sections for a reduced set of wavelengths (200 values) are shown (in the range of 250 to 280 nm). The resulting optimum sets of wavelengths are shown in table I. The units of f_v in this table are $1/\sigma$ where σ is in units of 10^{-18} cm^2 , that is, f_v has units of 10^{18} cm^{-2} . Since the error δR in Eq. (15) is unitless, the concentration error corresponding to $f_v=1$ is $\delta C \sim O(10^{18} \text{ cm}^{-2} \delta R)$. As an example, for $\delta R \sim 0.05$, $\delta C \sim 5 \times 10^{16} \text{ cm}^{-2}$, which corresponds to ~ 20 ppm-meters for a nominal air density of 2.5×10^{19} molecules/cm³. Of course one has to keep in mind that this is an absolute error and thus is a worst case estimate for a given estimate of δR . We should note that in some cases the optimum wavelengths are the same for more than one species as is the case for toluene and m-xylene in Table I. However, in some cases an optimum set for one species can be

far from optimum for another species. As an example of this situation, we find $f_v = 13.3$, if the optimum benzene wavelengths are used for p-xylene. On the other hand, we find that using the optimum toluene wavelengths for benzene and p-xylene results in f_v values which are remarkably close to optimum values for these two species (using toluene wavelengths we get $f_v = 0.57161$ for benzene compared to the optimum value of 0.57149, and $f_v = 0.52389$ for p-xylene compared to the optimum value of 0.52344). This issue is being further investigated to see if there is any mathematical basis for the existence of a global set of optimum wavelengths for all the species being considered.

The above method of finding optimum sets of wavelengths works well for a small number of species, but begins to be impractical for more than five species with 200 possible wavelength values. Also, as mentioned previously, there are possibly many other sets of wavelengths which have close to optimum f_v values. A simple method of finding such sets is to randomly choose sets of wavelengths in the desired range and then use the conjugate gradient method to find a local minimum of the functional f_v . By choosing a large enough number of random sets, it is likely that values very close to the optimum will be found. This method was implemented in a computer code which uses Powell's method as implemented in the Numerical Recipes routine POWELL⁽¹⁰⁾. After a local minimum is found, all wavelength values are perturbed (one at a time) by ± 0.2 nm and the search for the minimum is repeated. This is done to avoid the potential problem of local minima created by noise in the cross sections. The cross sections in Fig. (1) are used for the aromatic compounds and linear interpolation between wavelength values is used in order for f_v to be defined as a continuous function of the wavelengths throughout the domain. Table II shows the results of the best 5 sets of wavelengths (local minima) for each of the species, obtained by using 1000 random sets of 4 wavelengths each, in the range of 250-280nm. Many of these initial sets of random wavelengths result in the same local minimum values, however, such repeated values are not shown in the table. Because we use the full set of wavelengths as opposed to the reduced set used to obtain the results in Table I, it is possible and indeed we do find smaller values of f_v than those in Table I for all the cases considered. In addition to finding wavelength sets which are very close to the true global optimum, the speed of this method makes it very attractive from a practical point of view (for 4 species, CPU time was about 35 seconds to go through 1000 random sets of 4 wavelengths on a Sun SPARC 10 workstation).

Table I. Optimum wavelengths using an exhaustive global search

	λ_1	λ_2	λ_3	λ_4	f_v
Benzene	270.68	266.86	263.10	252.96	0.571
Toluene	272.28	270.68	266.86	252.96	0.867
M-xylene	272.28	270.68	266.86	252.96	1.061
P-xylene	272.28	270.68	260.44	252.96	0.523

Table II.

	λ_1	λ_2	λ_3	λ_4	f_v
Benzene	252.98	266.88	270.72	272.32	0.533
	"	263.14	266.88	270.72	0.533
	"	260.54	"	"	0.533
	"	263.86	"	270.73	0.533
	"	254.38	"	"	0.533
Toluene	252.98	266.88	270.72	272.34	0.858
	259.02	"	"	"	0.862
	252.98	"	271.14	"	0.867
	259.02	"	"	"	0.869
	252.98	263.90	266.88	"	0.878
M-xylene	252.98	266.86	270.72	272.32	1.002
	259.04	"	"	"	1.003
	254.00	"	"	"	1.013
	260.10	"	"	"	1.018
	252.98	260.38	270.72	"	1.041
P-xylene	260.54	266.88	270.72	272.32	0.454
	252.98	"	"	"	0.454
	254.00	"	"	"	0.454
	259.04	"	"	"	0.454
	263.14	"	"	"	0.454

The preceding results assumed that the error δR is independent of wavelength. In practical situations this is usually not the case for UV lidar because of the dependence of atmospheric attenuation on wavelength. Also, if large concentrations for one or more species are expected, the optimum wavelengths will need to be shifted away from absorption peaks in order to avoid near complete absorption. Also, because for some species there are very fast rising absorption bands, small errors in wavelength measurement can lead to large errors in the cross sections. To include this effect in the optimization process, the error given by equation (15) needs to be modified to:

$$\delta C_N = \left\langle \delta \underline{R}, \hat{\underline{\sigma}}_N \right\rangle / \left\langle \hat{\underline{\sigma}}_N, \hat{\underline{\sigma}}_N \right\rangle + \left\langle \underline{R}, \delta \left(\frac{\hat{\underline{\sigma}}_N}{\left\langle \hat{\underline{\sigma}}_N, \hat{\underline{\sigma}}_N \right\rangle} \right) \right\rangle \quad (20)$$

To account for effects of atmospheric attenuation and large concentrations we consider a more realistic analysis of the error $\delta R(\lambda)$ for the case of range resolved absorption lidar. If the backscatter intensity before and after the plume is given by $b(\lambda)$ and $a(\lambda)$ respectively, with associated errors $\delta b(\lambda)$ and $\delta a(\lambda)$, we have for small errors:

$$\delta R(\lambda) \approx \frac{1}{2} \left(\frac{\delta b}{b} - \frac{\delta a}{a} \right) \quad (21)$$

We can also write the signal levels before and after the plume as:

$$b(\lambda) = b_0(\lambda) \exp \left[-2 \Sigma_a(\lambda) R_p \right] \quad (22)$$

$$a(\lambda) = b(\lambda) \exp \left[-2 \sum_{k=1}^N \sigma_k(\lambda) C_k \right]$$

where b_0 is some reference signal amplitude, $\Sigma_a(\lambda)$ is the atmospheric attenuation coefficient, and R_p is the range to the plume. The factor of two accounts for the two way transmission of scattered light across the plume and the atmosphere. Since the signal level before the plume is larger than after the plume, and δb and δa are measurement errors, the δb error is at most of the same order as the δa error term, and thus we consider only the δa term. Thus using equation (22) we can write:

$$\delta R(\lambda) \approx \frac{\delta a(\lambda)}{b_0(\lambda)} \exp \left[2 \Sigma_a(\lambda) R_p + 2 \sum_{k=1}^N \sigma_k(\lambda) C_k \right] \quad (23)$$

If $\delta a(\lambda)/b_0(\lambda)$ is independent of λ and is equal to some constant δ_0 , then a reasonable criterion for minimizing the error in concentration of the N -th species can be written using equations (20) and (23) as:

$$g_v = \frac{\delta_0 \sum_{i=1}^v |\hat{\sigma}_N(\lambda_i)| \exp \left[2 \Sigma_a(\lambda_i) R_p + 2 \sum_{k=1}^N \sigma_k(\lambda_i) C_k \right]}{\left\langle \hat{\underline{\sigma}}_N, \hat{\underline{\sigma}}_N \right\rangle} + \sum_{i=1}^v \left| \delta \left(\frac{\hat{\sigma}_N(\lambda_i)}{\left\langle \hat{\underline{\sigma}}_N, \hat{\underline{\sigma}}_N \right\rangle} \right) \right| \quad (24)$$

where the wavelengths are chosen to minimize g_v , and we assumed that $R(\lambda) = O(1)$. In the above equation the term $\delta(\hat{\sigma}_N(\lambda_i) / \langle \hat{\sigma}_N, \hat{\sigma}_N \rangle)$ can be estimated as:

$$\delta\left(\frac{\hat{\sigma}_N(\lambda_i)}{\langle \hat{\sigma}_N, \hat{\sigma}_N \rangle}\right) \approx \max_j \left\{ \left| \frac{\hat{\sigma}_N(\lambda_i)}{\langle \hat{\sigma}_N, \hat{\sigma}_N \rangle} \right|_{\lambda+\delta\lambda_j} - \left| \frac{\hat{\sigma}_N(\lambda_i)}{\langle \hat{\sigma}_N, \hat{\sigma}_N \rangle} \right|_{\lambda-\delta\lambda_j} \right\}$$

where λ is the vector of wavelengths and $\delta\lambda_j$ is the uncertainty in the wavelength measurement. This error analysis is meant only as an illustration and similar analysis needs to be applied to the specific lidar system under consideration. One of the things that was not considered here but needs to be considered for a specific system is how the signal level, instrument gain setting and SNR are related. It is possible that a low signal with a high gain setting could have the same SNR as a high signal with a low gain setting. In such a situation, the effect of atmospheric attenuation on the error estimate might be significantly different from what we considered above.

V. Optimized Detection for Fluorescence Lidar

Given an excitation wavelength λ_i , the spectrally resolved fluorescence from an optically thin target can be written as:

$$M(\lambda_i, \lambda_j) = E_l(\lambda_i) C_o \sum_k C_k S_k(\lambda_i, \lambda_j) \quad (25)$$

where $M(\lambda_i, \lambda_j)$ denotes the measured fluorescence per unit λ_j , E_l is the laser energy, C_o is an overall normalization constant that takes into account the range to target and solid angle of the detector system as well as other factors, C_k is the concentration for k -th species (line integrated density) and $S_k(\lambda_i, \lambda_j)$ is the spectral signature which is written in terms of the constitutive physical quantities as:

$$S_k(\lambda_i, \lambda_j) = \frac{\lambda_i}{\lambda_j} \sigma_k(\lambda_i) q_k(\lambda_i) Q_k(\lambda_i) F_k(\lambda_i, \lambda_j) \quad (26)$$

where σ is the absorption cross section, q is the yield (time integrated probability of fluorescence emission, once a photon is absorbed), Q is fraction of fluorescence that is not quenched, and F is the spectral shape function normalized such that $\int d\lambda_j F_k(\lambda_i, \lambda_j)$ is unity. The effect of atmospheric attenuation can also be included in Eq. (25) by multiplying the spectral signatures by the attenuation factor given by: $\exp\left\{-\left[\Sigma_a(\lambda_i) + \Sigma_a(\lambda_j)\right]R_p\right\}$, where all the quantities are as defined previously.

Based on results of the previous sections, for N species, there are N pieces of information which are needed for minimizing the absolute error in the calculated concentration of a species in the presence of all the others. In the case of fluorescence, each piece of information is an excitation/fluorescence pair and the quantity to be minimized is the same as in Eq. (16), that is:

$$f_v = \sum_{p=1}^v \left| \hat{S}_N(\lambda_i, \lambda_j) \right| \left/ \sum_{p=1}^v \left[\hat{S}_N(\lambda_i, \lambda_j) \right]^2 \right. \quad (27)$$

with $v=N$ and p representing the λ_i, λ_j pairs. As in the case of absorption, it is possible to search for a global minimum of the above quantity by randomly choosing excitation/fluorescence pairs and then use the conjugate gradient method to find local minima. This of course requires knowledge of the functions in Eq. (26) in a continuous manner. In contrast to the absorption case, finding the optimum value of f_v requires minimization over the $2N$ dimensional space. This can be easily done if there are sufficient measurements to represent the variation of the functions in Eq. (26) over the wavelength range of interest. Another possible and more practical method of optimization is a two step approach. The first step involves finding optimum excitation wavelengths by considering the integrated fluorescence. This is done exactly in the same way as the absorption case except the product $\sigma_k(\lambda_i)q_k(\lambda_i)Q_k(\lambda_i)$ is used instead of the absorption cross sections. If the dependence of $q_k(\lambda_i)Q_k(\lambda_i)$ on wavelength is sufficiently weak, the results will be the same as for absorption optimization. If atmospheric attenuation is significant, then the product of $\sigma_k(\lambda_i)q_k(\lambda_i)Q_k(\lambda_i)$ and $\exp[-\sum_a(\lambda_i)R_p]$ should be used. The second step would then be to choose excitation/fluorescence pairs randomly and find local minima over the fluorescence wavelength range using the conjugate gradient method.

As a practical matter the spectrally resolved fluorescence might not be available during field measurements, but rather only the integrated fluorescence over certain spectral regions. Also, it might be possible to increase signal to noise ratio (SNR) by integrating the fluorescence over finite spectral regions. In this case the integrated spectra would be used and a set of optimum excitation/fluorescence bands would be obtained. The optimization over these pairs is done by minimizing the equivalent functional as given by equation (27). Since these pairs are now discrete, the search for the global minimum can be done by either going through all possible combinations (which is only practical for a small number of species) or by randomly picking pairs and searching for local minima by moving to adjacent points (in both the excitation and fluorescence dimensions) until a minimum value of the functional is obtained. A genetic algorithm could also be used for this search. For wide enough fluorescence bands the atmospheric attenuation correction needs to be applied to laboratory measured spectra before integration over these bands.

As an example of this process we consider finding the optimum excitation/fluorescence pairs for detection of the aromatic species used in the absorption example in the previous section. Fluorescence spectra for these species at near optimum absorption wavelengths are shown in Figs. (3-6). These spectra were measured in gas cells at low pressure and backfilled with air at normal atmospheric pressure⁽¹¹⁾. The fluorescence range at each excitation wavelength is divided into bands (3-5 bands are used) with the first wavelength set at $\lambda = \lambda_i + \Delta\lambda$, where λ_i is the excitation wavelength and $\Delta\lambda \approx 7.5$ nm is added to avoid overlap with the elastic scattering region (for measured data the elastic signal is subtracted and this is done only as a precaution). The bands for all the excitation wavelengths are shown superimposed on the spectra in the figures. This division is somewhat arbitrary and is possibly

not optimum, but the bands are chosen with large enough widths in order to get reasonable canceling of statistical noise. The width of the bands needs to be determined depending on the particular application in such a way so as to maximize signal to noise ratio. Spectra for the pairs are then obtained by integration of the original spectra over these bands and optimum pairs are found by using a global search. The table below shows the optimum pairs for each species. It should be noted that some of the optimum pairs are repeated for different species and there is a total of eight unique pairs for optimal detection of these species. We should also note that there are several other sets of pairs which have functional values which are very close to the optimum values.

The numerical examples given in this report do not account for the effect of atmospheric attenuation as well as many other effects to be encountered in a practical lidar system, and are given only as a means to illustrate the use of the method of orthogonal spectra. Calculations with effect of atmospheric attenuation included and application of optimized pairs to obtain solutions for field measurements are shown in reference (12).

Table III Optimum excitation/fluorescence pairs for detection of the aromatic species

	Band index	Excitation wavelength (nm)	Fluorescence range (nm)
Benzene	47	273.37	280.64 - 292.84
	33	266.88	274.17 - 286.37
	25	259.01	266.23 - 278.43
	7	252.95	272.41 - 284.61
Toluene	47	273.37	280.64 - 292.84
	41	271.21	278.43 - 290.63
	33	266.88	274.17 - 286.37
	25	259.01	266.23 - 278.43
M-xylene	47	273.37	280.64 - 292.84
	41	271.21	278.43 - 290.63
	25	259.01	266.23 - 278.43
	22	258.67	278.14 - 290.34
P-xylene	47	273.37	280.64 - 292.84
	44	271.47	278.73 - 290.92
	41	271.21	278.43 - 290.63
	33	266.88	274.17 - 286.37

VI. Summary

In this report we have considered the use of orthogonal spectra and cross sections as a quantitative measure of species distinguishability in mixtures and for lidar parameter optimization for both multispectral absorption and fluorescence lidar.

The orthogonal spectra are linear combinations of the original spectra and are obtained by the use of the Gram-Schmidt orthogonalization procedure for finite dimensional spaces. Using the orthogonal spectra for a specific species (orthogonal to all other potential species in a mixture) in a least squares solution for the concentrations amounts to isolating that species as if it were the only one present in the mixture. This means that the solution for the concentration of the species of interest can be written as a very simple expression which is only a function of the measured quantities and the orthogonal spectra (see equation (13)). This in turn makes the process of wavelength selection (excitation/fluorescence pairs in the case of fluorescence) for optimal detection a very clear and simple process. This is the case for both multispectral absorption and fluorescence lidar.

Using orthogonal spectra, a concise form for the absolute error in concentration is derived (see equations (15) and (16)). Optimized wavelengths for the detection of a specific species are defined to be those values that minimize the absolute error. It is shown by numerical analysis (mathematical proof is work in progress) that the optimum number of wavelengths (excitation/fluorescence pairs for fluorescence) is the same as the number of possible species in the mixture. A method is also described for finding the optimum sets of wavelengths. As stressed in the body of the report, once an optimum set of wavelengths is identified, measurements at these wavelengths need to be repeated as many times as possible in order to reduce statistical errors. Also several sets of near optimum wavelengths can be used to minimize potential systematic errors. The effects of atmospheric attenuation, large concentrations and uncertainties in wavelength measurement are also discussed and expressions for the absolute error, including these effects are derived.

Two examples, one for absorption lidar and the other for fluorescence lidar are given. In the first example, absorption wavelengths are calculated for optimal detection of four species: benzene, toluene, p-xylene and m-xylene in mixtures containing these four species. These wavelengths are found using an exhaustive search for the global minimum of the absolute error functional for each species. A second method is used in which random sets of wavelengths are selected followed by application of the conjugate gradient method to find local minima of the absolute error. It is shown by example that several near optimal sets of absorption wavelengths exist.

In the second example, optimization of fluorescence parameters is considered for detection of the four species considered in the absorption example. The fluorescence wavelength range is divided into a small number of bands for each excitation wavelength, and excitation/fluorescence pairs are found which minimize the absolute error (see equation (27)). These optimal pairs should result in best estimates of species concentrations in mixtures if there is a sufficient number of measurements to reduce statistical errors.

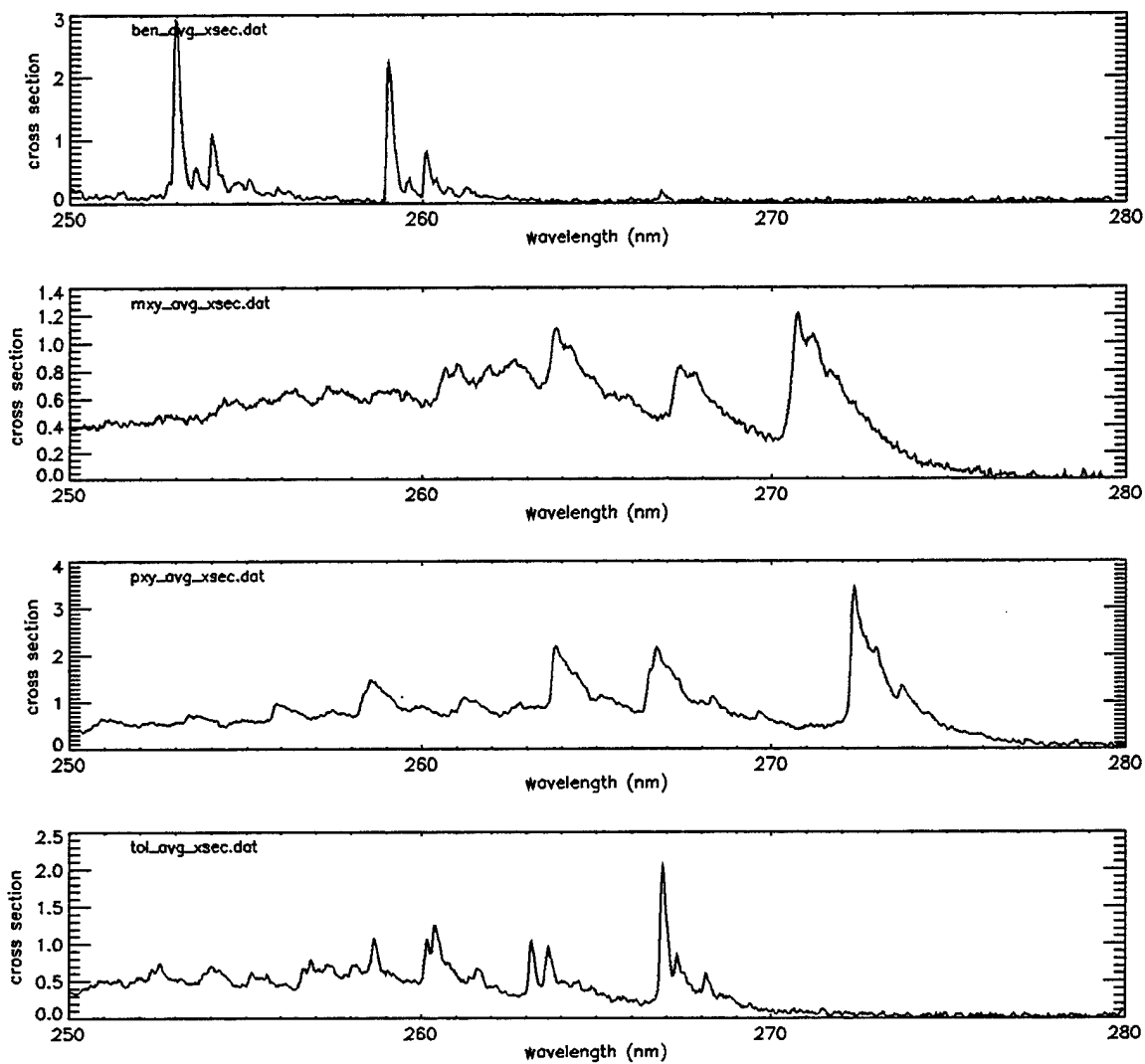


Fig. 1. Cross sections for the aromatic compounds. From top to bottom: benzene, m-xylene, p-xylene and toluene. The units are in 10^{-18} cm^2 .

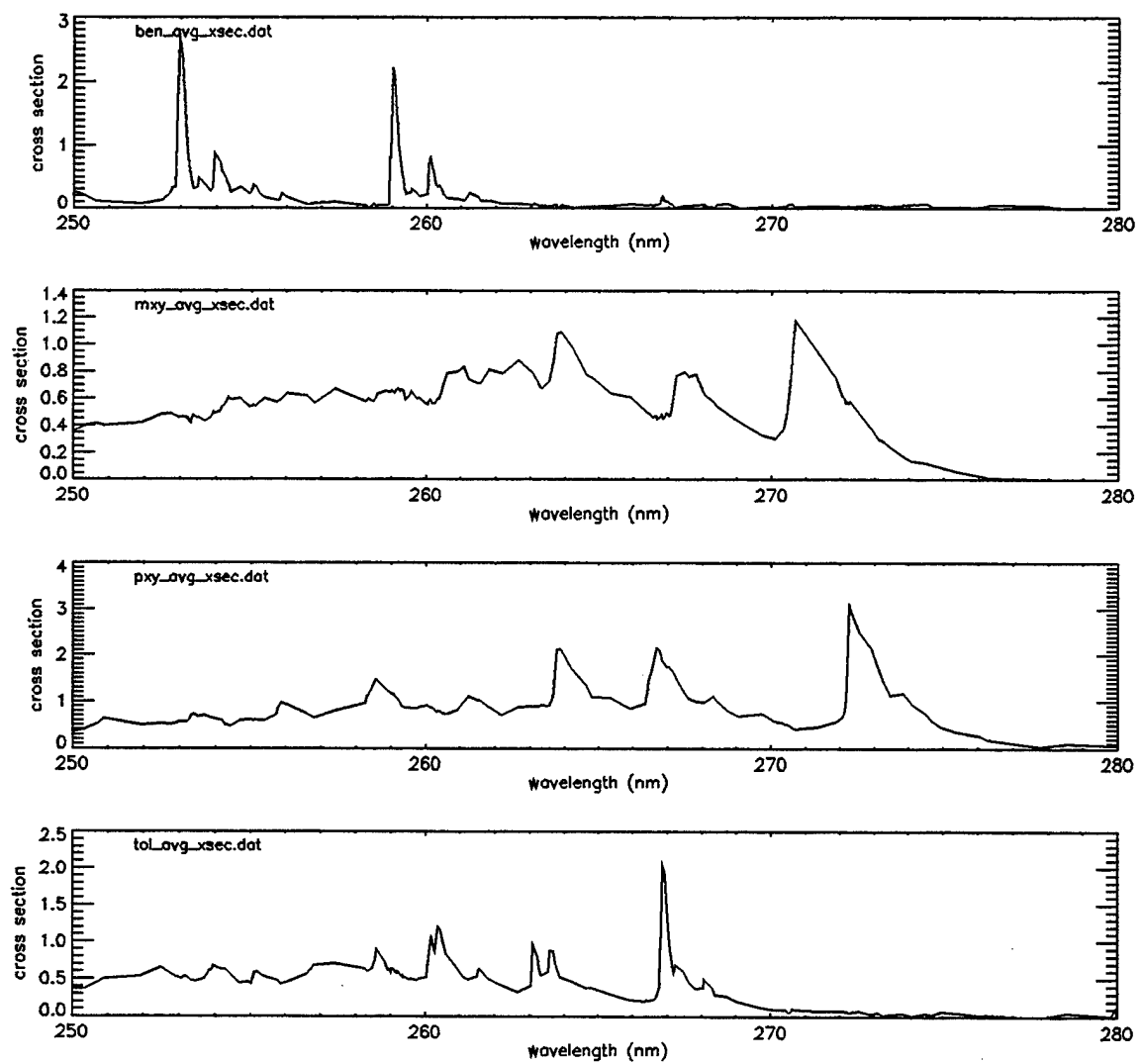


Fig. (2). Cross sections for reduced set of wavelengths. Same order and units as in Fig. (1).

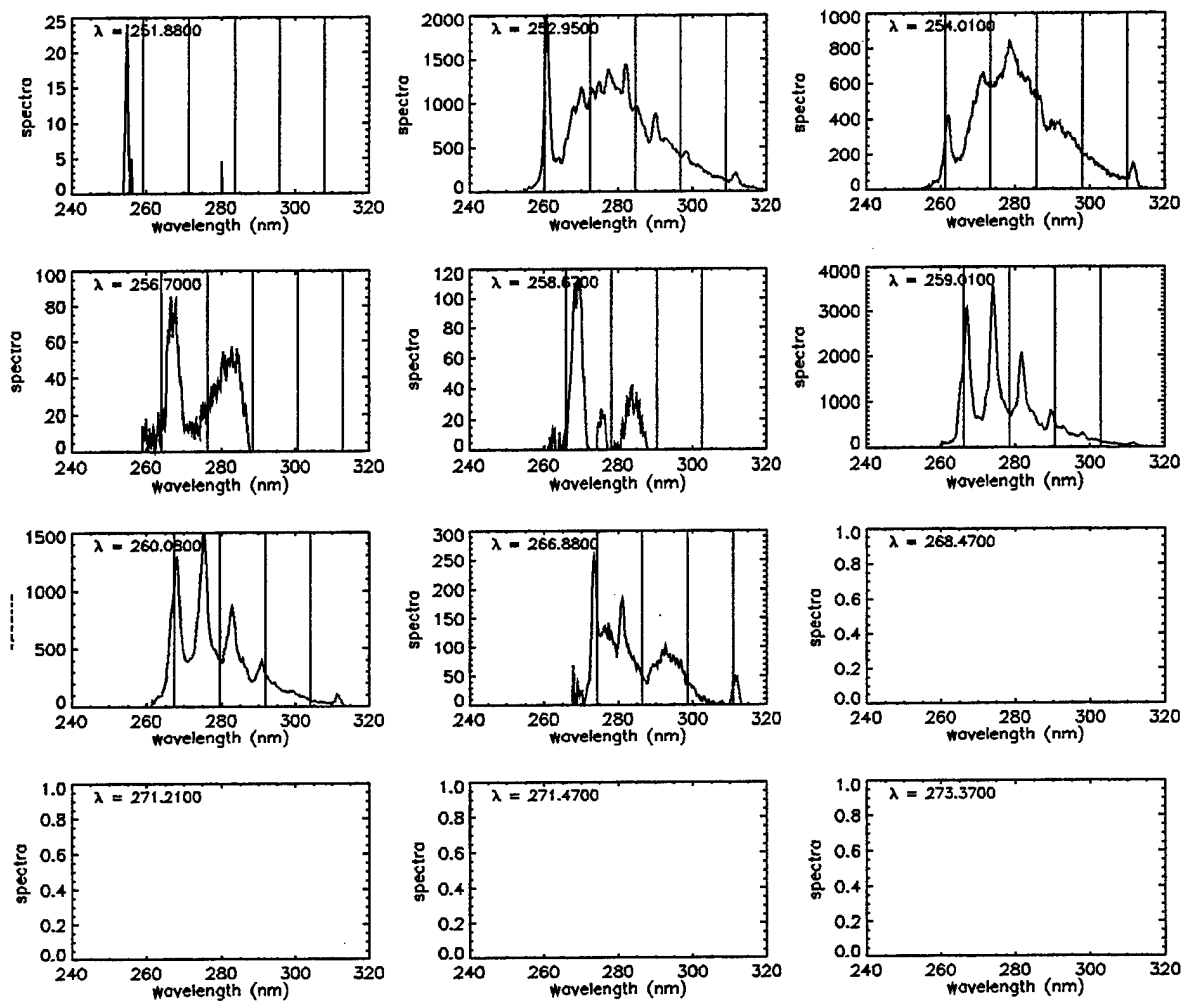


Fig. (3). Laboratory measured spectra for Benzene at different excitation wavelengths.

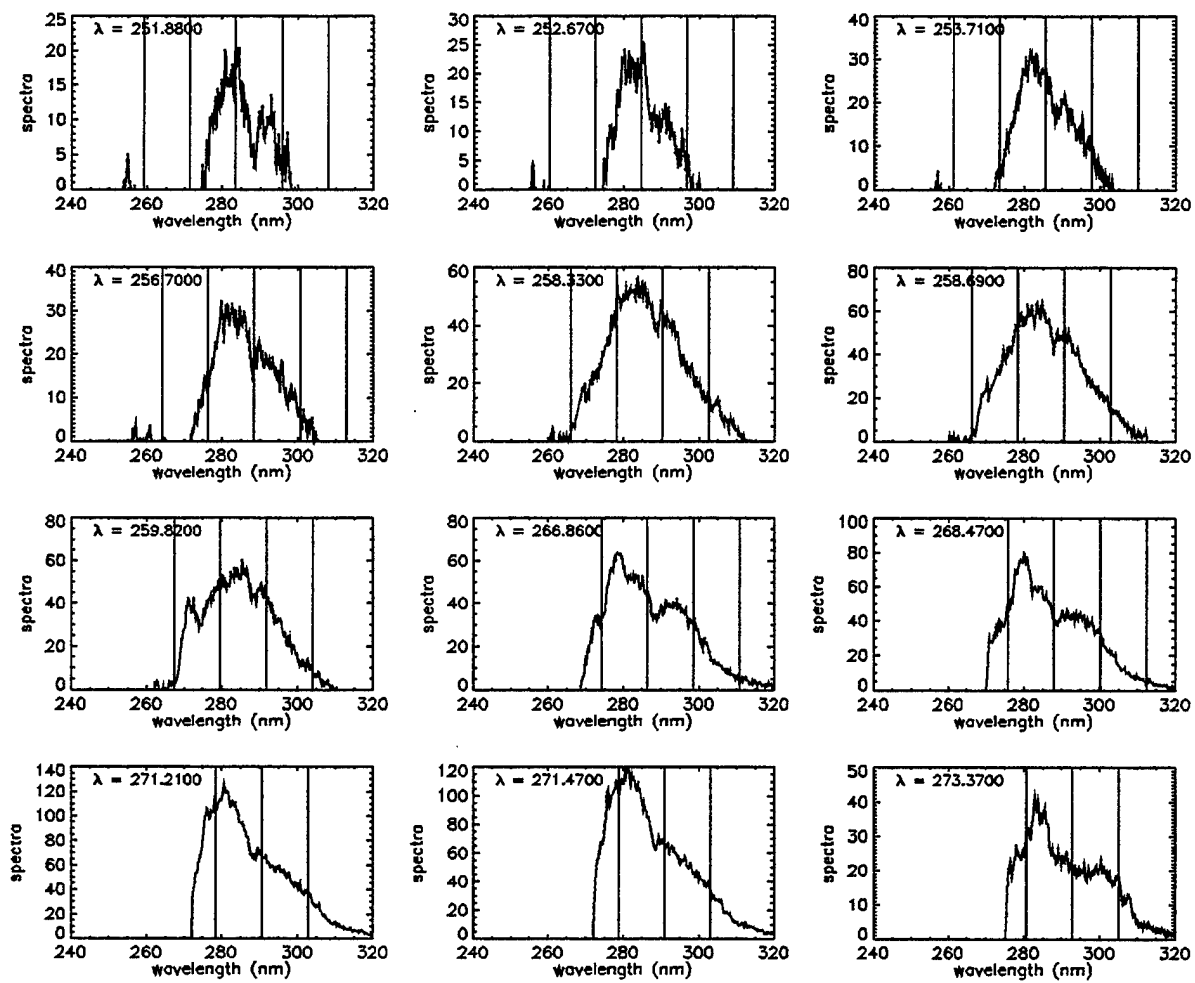


Fig. (4). Laboratory measured spectra for m-xylene.

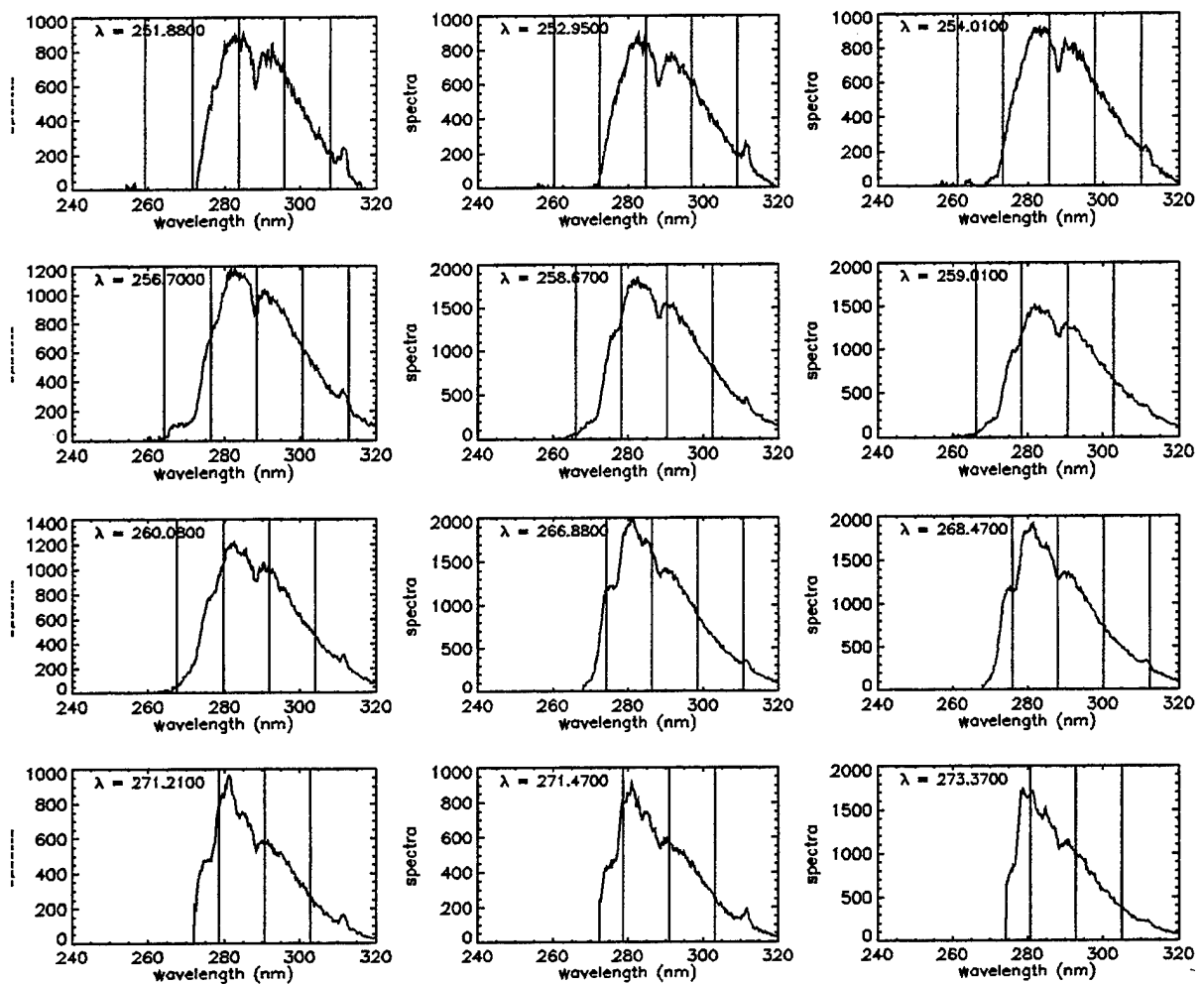


Fig. (5). Laboratory measured spectra for P-xylene

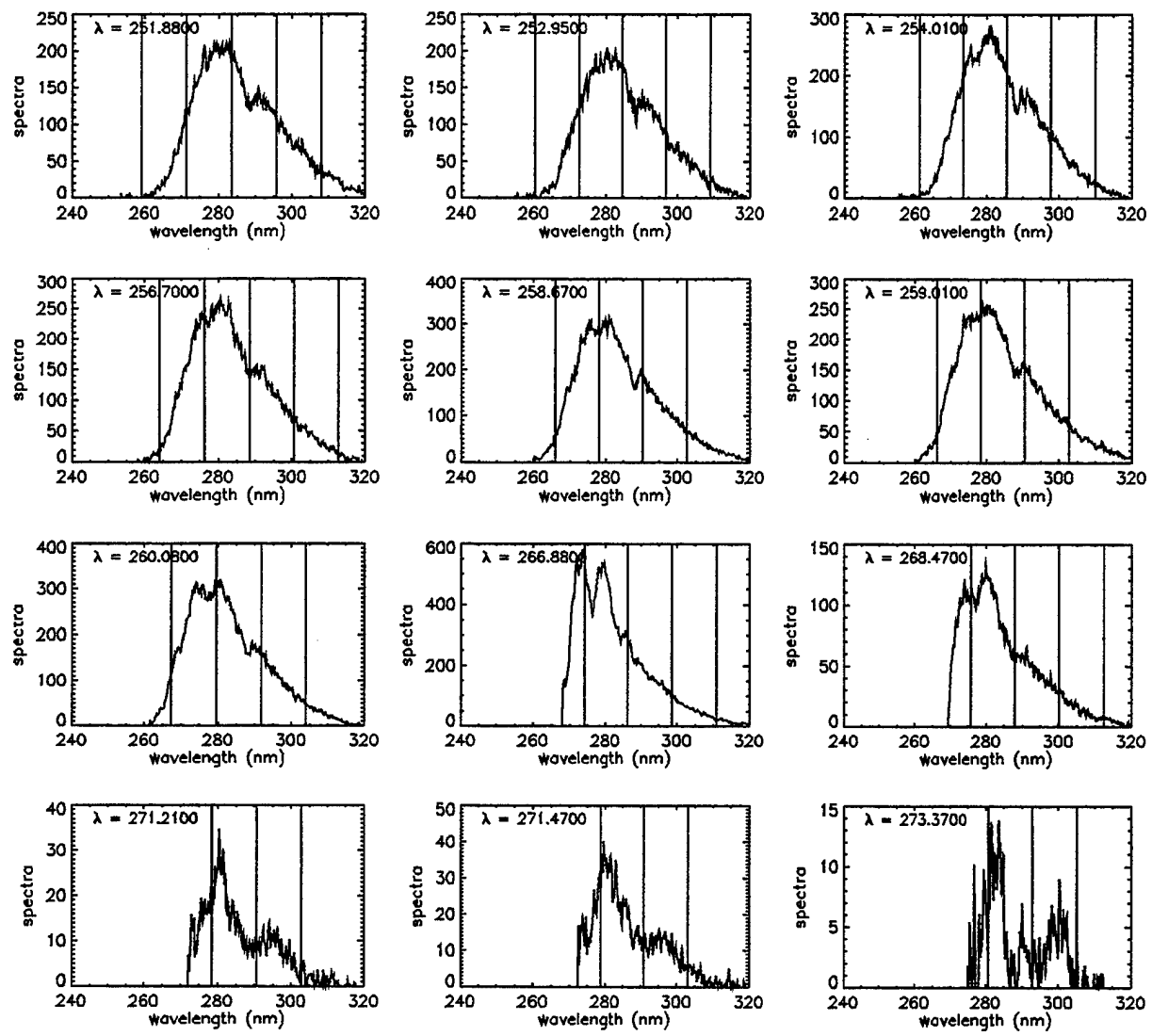


Fig. (6). Laboratory measured spectra for Toluene.

VII. References

1. P. J. Hargis, Jr., G. C. Tisone, T. D. Raymond, et al., "Integrated multispectral UV fluorescence and absorption lidar system for remote chemical analysis", SPIE Proceedings, Vol. 3127, 1997.
2. A. J. Ramponi, "MWIR lidar systems and multiline DIAL techniques", SPIE Proceedings, Vol. 3127, 1997.
3. C. R. Quick, Jr., "Development of a frequency-agile high-repetition-rate CO₂ DIAL system for long-range chemical remote sensing", SPIE Proceedings, Vol. 3127, 1997.
4. P. J. Hargis, Jr., G. C. Tisone, J. S. Wagner, T. D. Raymond, and T. L. Downey, "Multispectral Ultraviolet Fluorescence Lidar for Environmental Monitoring", SPIE Proceedings, Vol. 2366, 1994
5. J. S. Wagner, M. W. Trahan, W. E. Nelson, G. C. Tisone, and B. L. Preppernau, Computers in Physics, Vol. 10, No. 2, 114, (1996).
6. J. S. Wagner, Private Communication.
7. D. M. Haaland and E. V. Thomas, Anal. Chem, Vol. 60, 1193, (1988).
8. P. Geladi, and B. R. Kowalski, J. Chemom, Vol. 1, 19, (1987).
9. B. F. Clark, G. C. Tisone, and I. R. Shokair, Sandia Internal Memo, Feb. 1997.
10. W. H. Press, B. P. Flannery, S. A. Teukolsky and W. T. Vetterling, "Numerical Recipes, The Art of Scientific Computing", Cambridge University Press, 1986.
11. P. J. Hargis, Jr., Private communication.
12. I. R. Shokair, "Data Analysis Using Optimized Fluorescence Bands", Sandia Internal Memo, August, 1997.

External Distribution:

Beatty, Daniel
U.S. Department of Energy, NN-20
1000 Independence Ave SW
Washington, DC 20585-0420

Christesen, Steven
U. S. Army ERDEC
ATTN: SCBRD-RTE
APG, MD 21010-5423

Fox, Marsha
Phillips Laboratory PL/LIMI
3550 Aberdeen SE
Kirtland AFB, NM 87117-5776

Hylden, Jeffrey
U.S. Department of Energy, NN-20
1000 Independence Ave SW
Washington, DC 20585-0420

Kacenjar, Steve
Lockheed Martin
751 Vandenburg Road, B-A, R-37A30
King of Prussia, PA 19406

Ramponi, Albert
Lawrence Livermore National Laboratory
P.O. Box 808, L-183
Livermore, California 94551

Scharlemann, Ted
Lawrence Livermore National Laboratory
P.O. Box 808, L-183
Livermore, California 94551

Swegle, John
Lawrence Livermore National Laboratory
P.O. Box 808, L-387
Livermore, California 94551

Busch, George
Los Alamos National Laboratory
CST-1, MS E543
Los Alamos, NM 87545

Koskelo, Aaron
Los Alamos National Laboratory
CST-1, MS J565
Los Alamos, NM 87545

MacKerrow, Edward
Los Alamos National Laboratory
X-CM, MS E543
Los Alamos, NM 87545

McVey, Brian
Los Alamos National Laboratory
X-CM, MS F645
Los Alamos, NM 87545

Quagliano, John
Los Alamos National Laboratory
CST-3, MS E543
Los Alamos, NM 87545

Schultz, John
Los Alamos National Laboratory
CST-1, MS E543
Los Alamos, NM 87545

Internal Distribution:

1	MS 1423	G. N. Hays, 1128
1	MS 1423	P. J. Hargis, 1128
1	MS 1423	R. Schmitt, 1128
1	MS 0971	A. R. Lang, 5703
1	MS 0972	C. A. Boye, 5705
1	MS 0965	K. R. Lanes, 5711
1	MS 0980	S. M. Gentry, 5725
1	MS 0980	B. R. Stallard, 5725
1	MS 0980	J. G. Taylor, 5725
1	MS 9004	M. E. John, 8100
1	MS 9056	M. Lapp, 8102
1	MS 9201	S. P. Gordon, 8112
1	MS 9104	W. R. Bolton, 8120
1	MS 9103	D. W. Hahn, 8120
1	MS 9103	K. L. Schroder, 8120
1	MS 9103	D. A. Stephenson, 8120
1	MS 9056	L. Thorne, 8120
1	MS 9057	S. E. Bisson, 8366
1	MS 9057	T. J. Kulp, 8366
1	MS 1190	D. L. Cook, 9500
1	MS 1190	J. P. Quintenz, 9500
1	MS 1188	R. A. Hamil, 9512
1	MS 1188	D. E. Bliss, 9512
1	MS 1188	S. M. Cameron, 9512
1	MS 1188	P. C. Gray, 9512
15	MS 1188	I. R. Shokair, 9512
1	MS 1188	M. W. Trahan, 9512
1	MS 1188	J. S. Wagner, 9512
1	MS 1186	T. A. Mehlhorn, 9533
1	MS 1188	C. L. Olson, 9541
1	MS 1186	S. E. Rosenthal, 9573
1	MS 9018	Central Technical Files, 8940-2
5	MS 0899	Technical Library, 4916
2	MS 0619	Review & Approval Desk, 12690
		For DOE/OSTI

M98004180



Report Number (14) SAND--97-2321

Publ. Date (11)

199709

Sponsor Code (18)

DOE/ER, XF

UC Category (19)

UC-405, DOE/ER

DOE